



Contents lists available at ScienceDirect

Bioorganic & Medicinal Chemistry Letters

journal homepage: www.elsevier.com/locate/bmcl

A red-emitting naphthofluorescein-based fluorescent probe for selective detection of hydrogen peroxide in living cells

Aaron E. Albers, Bryan C. Dickinson, Evan W. Miller, Christopher J. Chang*

Department of Chemistry, University of California, 532A Latimer Hall, Berkeley, CA 94720, USA

ARTICLE INFO

Article history:

Received 21 June 2008

Revised 8 August 2008

Accepted 11 August 2008

Available online 14 August 2008

Keywords:

Fluorescent probe
Hydrogen peroxide
Naphthofluorescein
Flow cytometry
Near infrared

ABSTRACT

We report the synthesis, properties, and cellular application of Naphtho-Peroxyfluor-1 (NPF1), a new fluorescent indicator for hydrogen peroxide based on a red-emitting naphthofluorescein platform. Owing to its boronate cages, NPF1 features high selectivity for hydrogen peroxide over a panel of biologically relevant reactive oxygen species (ROS), including superoxide and nitric oxide, as well as excitation and emission profiles in the far-red region of the visible spectrum (>600 nm). Flow cytometry experiments in RAW264.7 macrophages establish that NPF1 can report changes in peroxide levels in living cells.

© 2008 Elsevier Ltd. All rights reserved.

The chemistry and biology of hydrogen peroxide (H_2O_2) is of current interest owing to its dual roles as a canonical marker for oxidative stress and as a newly recognized mediator for cellular signaling.^{1–7} Because the dynamic production, accumulation, and clearance of H_2O_2 in living systems can have disparate physiological and/or pathological consequences, new methodologies that allow selective and sensitive detection of this reactive oxygen metabolite in biological settings offer promise for helping to elucidate the complex contributions of peroxide to health, aging, and disease. Optical imaging with H_2O_2 -responsive emissive probes offers an attractive approach to this goal, and several systems for H_2O_2 visualization in biological samples have been reported recently, including those using small-molecule,^{8–17} protein,^{18,19} and nanoparticle,²⁰ reporters. In this context, luminescent indicators that possess excitation and emission profiles in the visible far-red to near-infrared region of the electromagnetic spectrum are highly desirable owing to reduced background interference from endogenous cellular components in this energy range, resulting in enhanced optical transparency of tissue and the ability to interrogate thicker specimens. In this report, we present the synthesis, spectroscopy, and live-cell evaluation of Naphtho-Peroxyfluor-1 (NPF1), a new small-molecule fluorescent probe for hydrogen peroxide based on a red-emitting naphthofluorescein dye platform. NPF1 utilizes a caged boronate switch to provide specific detection of H_2O_2 over competing reactive oxygen species (ROS), including superoxide, nitric oxide, and hydroxyl radical, and excitation and

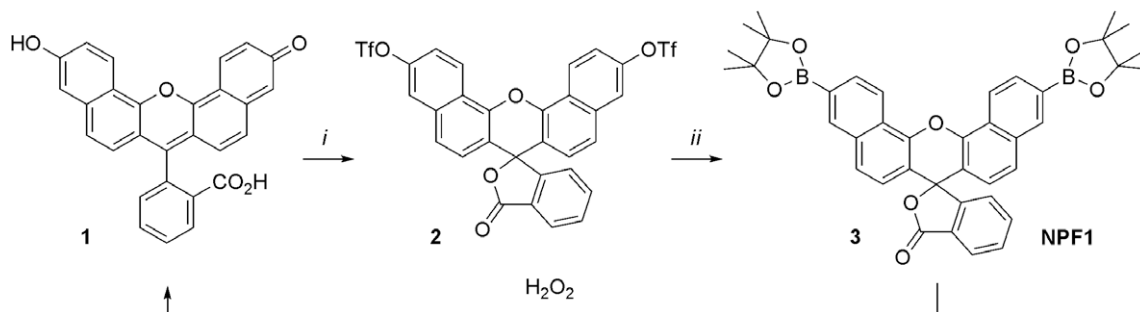
emission profiles in the visible far-red region (>600 nm). We further show that the red-emitting indicator is capable of reporting changes in H_2O_2 levels in living cells by flow cytometry.

Scheme 1 summarizes the design, synthesis, and activation of NPF1. Previous work from our laboratory established that the chemoselective conversion of aryl boronates to phenols provides a reaction-based approach to specific detection of H_2O_2 over other ROS.^{12–17} To extend this strategy to a system that possesses lower energy absorption/emission profiles, we turned our attention to fluorescein derivatives with extended naphthalene conjugation.^{21–25} In particular, we reasoned that appending boronates to the 4' and 9' positions of a naphthalene-expanded xanthenone scaffold would force this platform to adopt a closed, colorless, and non-fluorescent lactone form and furnish a caged, red-emitting naphthofluorescein compound that could be unmasked in the presence of H_2O_2 . Related sulfonate- and phosphinate-capped naphthofluorescein have been reported for fluorescence detection of peroxide,¹¹ and superoxide,²⁶ respectively. NPF1 is readily obtained in two steps from naphthofluorescein according to **Scheme 1**.

NPF1 was evaluated in aqueous solution at physiological pH (20 mM Hepes buffer, pH 7.5, 37 °C). In the absence of H_2O_2 , NPF1 displays no discernable absorption or emission bands in the visible region of the spectrum, as expected for the parent compound in the closed lactone form. The compound does possess an absorption in the ultraviolet region due to the naphthalene chromophore ($\lambda_{\text{max}} = 345$ nm, $\epsilon = 2.24 \times 10^4 \text{ M}^{-1} \text{ cm}^{-1}$). Treatment of NPF1 with H_2O_2 triggers an increase in red-colored fluorescence centered at 660 nm with concomitant growth of an absorption

* Corresponding author. Tel.: +1 510 642 4704; fax: +1 510 642 7301.

E-mail address: chrischang@berkeley.edu (C.J. Chang).



Scheme 1. Synthesis and activation of Naphtho-Peroxyfluor-1 (NPF1). Reagents and conditions: (i) *N*-phenyl-bis(trifluoromethanesulfonylimide), DIPEA, DMF, 25 °C, 24 h; (ii) Pd(dppf)Cl₂·CH₂Cl₂, dppf, bis(pinacolato)diboron, KOAc, 1,4-dioxane, 100 °C, 24 h.

feature centered at 598 nm characteristic of the ring-opened naphthofluorescein product.^{25,27} Figure 1 shows the fluorescence response of NPF1 to H₂O₂ from 0 to 60 min. NPF1 exhibits a >25-fold increase in emission intensity after H₂O₂ treatment under these conditions. We note that deprotections of NPF1 are kinetically controlled and are not complete at these early time points. NPF1 is highly specific for H₂O₂ over competing ROS. Figure 2 shows the relative reactivities of the indicator toward various oxidants. NPF1 is selective for H₂O₂ over a variety of reactive oxygen and nitrogen metabolites, including superoxide, nitric oxide, hy-

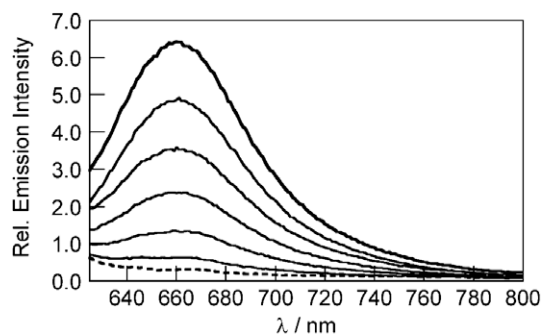


Figure 1. Fluorescence response of 5 μM NPF1 to 100 μM H₂O₂. The dashed spectrum was acquired before H₂O₂ addition (dotted line) and the solid line spectra shown were acquired after 10, 20, 30, 40, 50 and 60 min incubation with H₂O₂. Spectra were acquired in 20 mM Hepes, pH 7.5, at 37 °C (λ_{exc} = 598 nm).

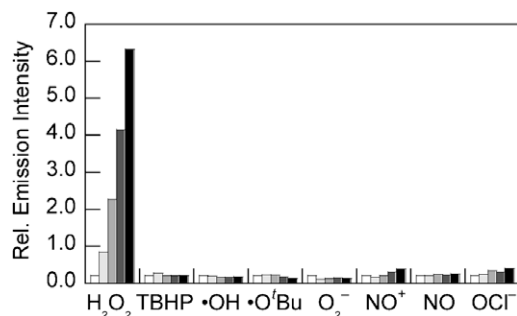


Figure 2. Fluorescence responses of 5 μM NPF1 to 100 μM reactive oxygen species (ROS). Hydrogen peroxide (H₂O₂), *tert*-butyl hydroperoxide (TBHP), and hypochlorite (OCl⁻) were delivered from 30%, 70%, and 5% aqueous solutions, respectively. Hydroxyl radical (·OH) and *tert*-butoxy radical (·O[•]Bu) were generated by reactions of 1 mM Fe²⁺ with 100 μM H₂O₂ or 100 μM TBHP, respectively. Superoxide (O₂^{•-}) was generated enzymatically using a xanthine/xanthine oxidase system. NO[•] was delivered using *S*-nitrosocysteine (SNOC). NO was delivered using NOC-5. Spectra were acquired in 20 mM Hepes, pH 7.5, and all data were obtained after incubation with the appropriate ROS at 37 °C. Bars represent relative emission responses (λ_{exc} = 598 nm, λ_{em} = 660 nm) at 0 (white), 15 (light gray), 30 (gray), 45 (dark gray), and 60 min (black) after addition of the appropriate ROS.

droxyl radical, and *tert*-butyl hydroperoxide. Kinetics measurements of the fluorescence response of NPF1 to H₂O₂ under pseudo-first-order conditions (1 μM NPF1, 1 mM H₂O₂) give an observed rate constant of $k_{\text{obs}} = 3.1(1) \times 10^{-4} \text{ s}^{-1}$ (Fig. 3).

With spectroscopic data demonstrating the H₂O₂-specific response of NPF1 in aqueous media at physiological pH, we turned our attention to evaluating the ability of the dye to report changes in H₂O₂ levels in live-cell systems. To this end, RAW264.7 macrophages were treated with either (i) 20 μM NPF1 only for 2 h at 37 °C or (ii) 20 μM NPF1 for 1 h followed by 100 μM H₂O₂ for an additional 1 h at 37 °C, and the relative fluorescence intensities of these cells were analyzed by flow cytometry. A clear population shift is observed in cells exposed to H₂O₂ compared to control cells without H₂O₂ exposure, with the H₂O₂-treated cells displaying a marked increase in red-colored fluorescence over their untreated counterparts (Fig. 4). Dynamic light scattering measurements also confirm that the cells are viable throughout the experiments (Supplementary data). As observed for other diboronate reagents,¹⁵ initial attempts to use NPF1 for intracellular H₂O₂ detection under oxidative signaling conditions were unsuccessful, and confocal microscopy measurements were also hampered by the relative dimness of the naphthofluorescein product relative to fluorescein.^{25,27} Nevertheless, these results establish that NPF1 is cell-permeable and is capable of responding to intracellular changes in H₂O₂ levels in living mammalian cells.

In summary, we have described a new boronate-based red-emitting fluorescent indicator for hydrogen peroxide in living cells. NPF1 possesses good selectivity for H₂O₂ over competing ROS, far-red visible excitation and emission profiles, and is capable of responding to changes in H₂O₂ levels within living cells. Ongoing and future efforts are focused on utilizing NPF1 and analogs for studies of peroxide biology in situations of oxidative stress, as well

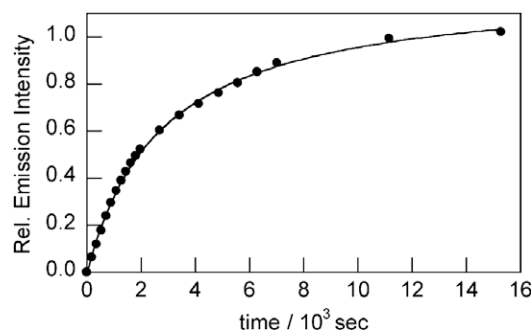


Figure 3. Time-course kinetics measurement of the fluorescence response of NPF1 to H₂O₂. Data were collected under pseudo-first-order conditions (1 μM NPF1, 1 mM H₂O₂). Spectra were acquired in 20 mM Hepes, pH 7.5, at 25 °C (λ_{exc} = 598 nm, λ_{em} = 660 nm), and data are plotted as relative emission intensities over initial background.

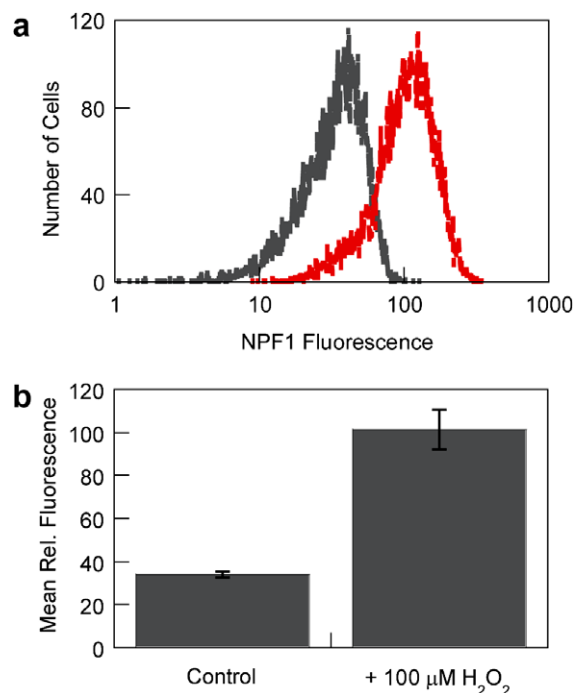


Figure 4. Flow cytometry analysis of NPF1-loaded live RAW264.7 macrophages in response to increases in H_2O_2 levels. Two aliquots of cells were incubated with $20\ \mu\text{M}$ NPF1 for 1 h. $100\ \mu\text{M}$ H_2O_2 was subsequently added to one of the aliquots, and the cells were incubated for an additional 1 h. Cells were then analyzed by flow cytometry. (a) Representative flow cytometry trace from one experiment described above. Data are shown for NPF1-loaded control cells in the absence of H_2O_2 (gray) and cells treated with H_2O_2 (red). (b) Mean relative fluorescence for populations shown in panel (a) from three replicate experiments. Error bars represent the standard deviation from the mean for the three experiments. The data represent at least 10,000 cells for each analysis.

as increasing the sensitivity and optical brightness of probes that emit in the far-red visible and near-infrared region for use in live-cell and in vivo imaging applications.

Acknowledgments

We thank the Beckman, Packard, and Sloan Foundations, and the NIH (GM 79465) for providing funding for this work. A.E.A., B.C.D., and E.W.M. thank the NIH Chemical Biology Graduate Program (T32 GM066698) for support. A.E.A. thanks the ACS Organic Division for an Emmanuil Troyansky Graduate Fellowship and UC Berkeley for a Chancellor's Opportunity Fellowship. E.W.M.

acknowledges a Stauffer fellowship for support. We thank Ann Fischer (UCB Tissue Culture Facility) for expert technical assistance and Prof. Carolyn Bertozzi for use of her laboratory's flow cytometer.

Supplementary data

Supplementary data associated with this article can be found, in the online version, at doi:10.1016/j.bmcl.2008.08.035.

References and notes

- Rhee, S. G. *Science* **2006**, 312, 1882.
- Stone, J. R.; Yang, S. *Antioxid. Redox Signal.* **2006**, 8, 243.
- Veal, E. A.; Day, A. M.; Morgan, B. A. *Mol. Cell* **2007**, 26, 1.
- D'Autréaux, B.; Toledano, M. B. *Nat. Rev. Mol. Cell Biol.* **2007**, 8, 813.
- Giorgio, M.; Trinei, M.; Migliaccio, E.; Pelicci, P. G. *Nat. Rev. Mol. Cell Biol.* **2007**, 8, 722.
- Poole, L. B.; Nelson, K. J. *Curr. Opin. Chem. Biol.* **2008**, 12, 18.
- Miller, E. W.; Chang, C. J. *Curr. Opin. Chem. Biol.* **2007**, 11, 620.
- Hempel, S. L.; Buettner, G. R.; O'Malley, Y. Q.; Wessels, D. A.; Flaherty, D. M. *Free Radic. Biol. Med.* **1999**, 27, 146.
- Soh, N. *Anal. Bioanal. Chem.* **2006**, 386, 532.
- Maeda, H.; Futkuyasu, Y.; Yoshida, S.; Fukuda, M.; Saeki, K.; Matsuno, H.; Yamauchi, Y.; Yoshida, K.; Hirata, K.; Miyamoto, K. *Agnew. Chem., Int. Ed.* **2004**, 43, 2389.
- Xu, K.; Huang, B.; Tang, H.; Yang, G.; Chen, Z.; Li, P.; An, L. *Chem. Commun.* **2005**, 5974.
- Chang, M. C. Y.; Pralle, A.; Isacoff, E. Y.; Chang, C. J. *J. Am. Chem. Soc.* **2004**, 126, 15392.
- Miller, E. W.; Albers, A. E.; Pralle, A.; Isacoff, E. Y.; Chang, C. J. *J. Am. Chem. Soc.* **2005**, 127, 16652.
- Albers, A. E.; Okreglak, V. S.; Chang, C. J. *J. Am. Chem. Soc.* **2006**, 128, 9640.
- Miller, E. W.; Tulyathan, O.; Isacoff, E. Y.; Chang, C. J. *Nat. Chem. Biol.* **2007**, 3, 263.
- Srikun, D.; Miller, E. W.; Domaille, D. W.; Chang, C. J. *J. Am. Chem. Soc.* **2008**, 130, 4596.
- Dickinson, B. C.; Chang, C. J. *J. Am. Chem. Soc.* **2008**, 130, 9638.
- Zhou, M.; Diwu, Z.; Panchuk-Voloshina, N.; Haugland, R. P. *Anal. Biochem.* **1997**, 253, 162.
- Belousov, V. V.; Fradkov, A. F.; Lukyanov, K. A.; Staroverov, D. B.; Shakhbazov, K. S.; Tersikh, A. V.; Lukyanov, S. *Nat. Methods* **2006**, 3, 281.
- Lee, D.; Khaja, S.; Velasquez-Castano, J. C.; Dasari, M.; Sun, C.; Petros, J.; Taylor, W. R.; Murthy, N. *Nat. Mater.* **2007**, 6, 765–769.
- For some recent selected examples see Hilderbrand, S. A.; Weissleder, R. *Tetrahedron Lett.* **2007**, 48, 4383. and references 22–26.
- Clark, M. A.; Hilderbrand, S. A.; Lippard, S. J. *Tetrahedron Lett.* **2004**, 45, 7129.
- Yang, Y.; Lowry, M.; Schowalter, C. M.; Fakayode, S. O.; Escobedo, J. O.; Xu, X.; Zhang, H.; Jensen, T. J.; Fronczek, F. R.; Warner, I. M.; Strongin, R. M. *J. Am. Chem. Soc.* **2006**, 128, 14081.
- Yang, Y.; Lowry, M.; Xu, X.; Escobedo, J. O.; Sibrian-Vazquez; Wong, L.; Schowalter, C. M.; Jensen, T. J.; Fronczek, F. R.; Warner, I. M.; Strongin, R. M. *Proc. Nat. Acad. Sci. U.S.A.* **2008**, 105, 8829.
- Lee, L. U.S. Patent 4933,471, 1990.
- Xu, K.; Liu, X.; Tang, B. *ChemBioChem* **2007**, 8, 453.
- Haugland, R. P. In *The Handbook: A Guide to Fluorescent Probes and Labeling Technologies*, 10th ed., Spence, M. T. Z. Ed.; Invitrogen Corp.: Carlsbad, CA, 2005.